Open access • Journal Article • DOI:10.1038/NMAT2250

Drug-sensing hydrogels for the inducible release of biopharmaceuticals.

Martin Ehrbar, Ronald Schoenmakers, Erik H. Christen, Martin Fussenegger ...+1 more authors

Institutions: University of Zurich, ETH Zurich

Published on: 10 Aug 2008 - Nature Materials (Nature Publishing Group)

Topics: Self-healing hydrogels and Novobiocin

Drug-sensing hydrogels for the inducible release of biopharmaceuticals

Ehrbar, M; Schoenmakers, R; Christen, E H; Fussenegger, M; Weber, W

Drug-sensing hydrogels for the inducible release of biopharmaceuticals

Abstract

Drug-dependent dissociation or association of cellular receptors represents a potent pharmacologic mode of action for regulating cell fate and function. Transferring the knowledge of pharmacologically triggered protein-protein interactions to materials science will enable novel design concepts for stimuli-sensing smart hydrogels. Here, we show the design and validation of an antibiotic-sensing hydrogel for the trigger-inducible release of human vascular endothelial growth factor. Genetically engineered bacterial gyrase subunit B (GyrB) (ref. 4) coupled to polyacrylamide was dimerized by the addition of the aminocoumarin antibiotic coumermycin, resulting in hydrogel formation. Addition of increasing concentrations of clinically validated novobiocin (Albamycin) dissociated the GyrB subunits, thereby resulting in dissociation of the hydrogel and dose- and time-dependent liberation of the entrapped protein pharmaceutical VEGF(121) for triggering proliferation of human umbilical vein endothelial cells. Pharmacologically controlled hydrogels have the potential to fulfil the promises of stimuli-sensing materials as smart devices for spatiotemporally controlled delivery of drugs within the patient.

Drug-sensing Hydrogels for the Inducible Release of Biopharmaceuticals

Martin Ehrbar[2], Ronald Schoenmakers[1], Erik H. Christen[1], Martin Fussenegger[1] and Wilfried Weber[1*]

[1]Department of Biosystems Science and Engineering, ETH Zurich, Mattenstrasse 26, 4058 Basel, Switzerland.

[2]Department of Cranio-Maxillofacial Surgery, University Hospital Zurich, Frauenklinikstrasse 24, 8091 Zurich, Switzerland.

[*]Correspondence should be addressed to WW: Phone: +41 44 633 63 50, Fax: +41 44 633 12 27, Email: wilfried.weber@bsse.ethz.ch

Drug-dependent dissociation or association of cellular receptors represents a potent pharmacologic mode of action for regulating cell fate and function[1, 2]. Transferring the knowledge of pharmacologically-triggered protein-protein interactions to material science will enable novel design concepts for stimuli-sensing smart hydrogels. Here we show the design and validation of an antibiotic-sensing hydrogel for the trigger-inducible release of human vascular endothelial growth factor[3]. Genetically engineered bacterial gyrase subunit B (GyrB[4]) coupled to polyacrylamide was dimerized by the addition of the aminocoumarin antibiotic coumermycin resulting in hydrogel formation. Addition of increasing concentrations of clinically validated novobiocin (Albamycin®) dissociated the GyrB subunits thereby resulting in dissociation of the hydrogel and dose- and time-dependent liberation of the entrapped protein pharmaceutical $VEGF_{121}$ for triggering proliferation of human umbilical vein endothelial cells. Pharmacologically-controlled hydrogels have the potential to fulfill the promises of stimuli-sensing materials[5-9] as smart devices for spatiotemporally controlled delivery of drugs within the patient.

Stimuli-sensing hydrogels responsive to enzymes[9-12], temperature[8], light[6], calcium[5], antigens[7] and DNA[13] hold great promises as smart materials for drug delivery within the body (reviewed in [14]), for tissue engineering[15] or as (nano-) valves in microfluidic applications[16]. Such materials commonly respond to triggers, which are difficult to apply in a patient background in the case of physical stimuli (e.g. light, temperature) or in the case of molecule-based stimuli due to stimulus concentrations hardly achievable in a physiologic background (e.g. antibody concentrations in the g/l range[7]). In contrast, the mode of action for pharmaceutical substances is designed to

occur within physiologic limits and therefore, hydrogels based on a pharmacologic mode of action are expected to show high compliance with future therapeutic applications.

For designing a hydrogel relying on a pharmacologic mode of action, we used the aminocoumarin antibiotic-dependent inhibition of bacterial gyrase, a potent target in combating microbial pathogens[17]. The antibiotic-responsive gel is based on polyacrylamide grafted with bacterial gyrase subunit B (GyrB), which can be dimerized by the aminocoumarin antibiotic coumermycin (+ Coumermycin), thereby resulting in gelation and three-dimensional stabilization of the hydrogel (Fig. 1a). Upon addition of the aminocoumarin novobiocin (Albamacin®, + Novobiocin), the interaction between GyrB and coumermycin is competitively inhibited, the three-dimensional structure is loosened and the hydrogel changes to the sol-state (Fig. 1a). Both antibiotics bind to GyrB with a similar dissociation constant enabling an efficient exchange of both antibiotic species ($K_d \approx 10^{-8}$ M, the relative binding constants of the antibiotics to GyrB are discussed controversially[18]).

As polymer we selected polyacrylamide functionalized with nitrilotriacetic acid (NTA) for chelating Ni^{2+} ions to bind hexahistidine-tagged (His_6) GyrB (Fig. 1b). For construction of the polymer, 2,2'-(5-acrylamido-1-carboxypentylazanediyl)diacetic acid (NTA-AAm) was synthesized (Supplementary Fig. 1 and Supplementary Fig. 2a for synthesis strategy and ^{1}H and ^{13}C NMR data), co-polymerized with acrylamide (AAm, Supplementary Fig. 2a) and the NTA groups were charged with Ni^{2+}. The molecular mass averages of the resulting polymer, poly(AAm-co-Ni^{2+}-NTA-AAm), as determined by gel permeation chromatography, are Mw = 74.10 kDa (weight average molecular weight) and Mn = 11.91 kDa (number average molecular weight) resulting in a polydispersity index D = 6.22. The molar mass peak maximum is Mp =

45.4 kDa. poly(AAm-co-Ni^{2+}-NTA-AAm) contains one NTA-AAm group per four acrylamide monomers as deduced from ^{1}H NMR analysis (Supplementary Fig. 2b) and reflecting the stoichiometry in synthesis.

The gene for *E.coli* gyrase subunit B (*gyrB*) was tagged with the coding sequence for six histidine residues. The coding region was placed under the control of the phage T_7-derived promoter and expressed in *E.coli* as a soluble cytoplasmatic protein. GyrB was purified via the hexahistidine tag using Ni^{2+}-based affinity chromatography (Supplementary Fig. 3a). Coumermycin-induced dimerization of genetically engineered GyrB was evaluated by incubating the protein in the presence of increasing coumermycin concentrations with subsequent addition of the amine-specific bifunctional crosslinking agent dimethylsuberimidate (DMS) and analysis of the complexes on denaturing polyacrylamide gel electrophoresis (Supplementary Fig. 3b). At a molar ratio of coumermycin : GyrB = 0.5, the strongest dimer formation (migrating at 54 kDa) could be observed in agreement with previous studies using non-engineered GyrB[18]. In order to exclude that the remaining band migrating at 27 kDa in the presence of 0.5 moles coumermycin per mol GyrB resulted from inefficient antibiotic-mediated GyrB dimerization but rather from incomplete DMS-mediated covalent crosslinking[18], we performed ultrafiltration experiments. GyrB was incubated in the presence or absence of coumermycin and subjected to ultrafiltration using a 50 kDa molecular weight cut-off filter. GyrB in the absence of coumermycin passed the filter efficiently (54 % of protein in filtrate), whereas only background GyrB levels could be detected in the filtrate, when coumermycin-dimerized GyrB was loaded (2.8 % of protein in filtrate) indicating that coumermycin-mediated GyrB dimerization was quantitative.

Synthesis of coumermycin-crosslinked hydrogels was performed by incubating hexahistidine-tagged GyrB in the absence or presence of coumermycin (1 mol coumermycin per 2 moles GyrB) or with a ten-fold molar excess of novobiocin. The protein was subsequently mixed with poly(AAm-co-Ni^{2+}-NTA-AAm) at a ratio of one GyrB per 11 Ni^{2+} ions chelated in the polymer. The solutions which all became viscous were incubated in PBS for 12 h prior to quantification of GyrB-polymer complexes released into the buffer (Fig. 2a). In the absence of coumermycin or in the presence of novobiocin, the viscous structures were completely dissolved and GyrB was quantitatively retrieved in the buffer. However, in the presence of coumermycin, only 13 ± 1 % of the GyrB was released into the buffer and a hydrogel was observed with an equilibrium degree of swelling to 146 ± 4 % of its initial volume thereby demonstrating the gelling effect of this dimerizing antibiotic (Fig. 2a).

In order to demonstrate that the hydrogel formation was effectively due to GyrB dimerization, we synthesized hydrogels using coumermycin-dimerized GyrB as above or coumermycin-dimerized GyrB which had further been covalently crosslinked by dimethylsuberimidate (DMS, crosslinking ratio: 33 ± 4 % as judged from SDS-PAGE analysis, data not shown). Following swelling for 12 h in PBS, the hydrogels were incubated in PBS containing 1 mM novobiocin and hydrogel dissolution was monitored by the release of GyrB-polymer complexes into the buffer (Fig. 2b). While coumermycin-crosslinked hydrogels were dissolved after 11 h in the presence of novobiocin, hydrogels with DMS-crosslinked GyrB (+ DMS) were stable for the observation period of 31 h (Fig. 2b). This observation confirms that the hydrogel was effectively formed by coumermycin-mediated dimerization of GyrB, which could be reversed by excess novobiocin. Instead of dissolving, DMS-stabilized hydrogels were swelling in response to the addition of novobiocin (Fig. 2c), which is reflecting the

drug-induced elimination of coumermycin-mediated crosslinks while the covalent crosslinks sustained the overall gel structure (Supplementary Fig. 4).

The gel characteristics were determined by small-strain oscillatory shear rheometry for hydrogels with and without covalent DMS crosslinks as described above and for hydrogels constructed by first mixing GyrB with poly(AAm-co-Ni^{2+}-NTA-AAm) and subsequent addition of the dimerizing antibiotic coumermycin (Fig. 2d). In all configurations hydrogels were obtained as is evident from storage moduli G' substantially exceeding loss moduli G'' (at 1 Hz), typical of crosslinked polymer networks[19]. A storage modulus of G' ≈ 1000 Pa was measured when GyrB was dimerized with coumermycin (and optionally DMS) prior to the mixing with poly(AAm-co-Ni^{2+}-NTA-AAm) (Fig. 2d). When the GyrB-poly(AAm-co-Ni^{2+}-NTA-AAm) complex was supplemented with dimerizing coumermycin at a later time point, a significantly lower storage modulus (G' = 284 ± 105, at a frequency of 1 Hz) was observed (Fig. 2d). This difference might reflect sterically hindered dimerization of GyrB already bound to poly(AAm-co-Ni^{2+}-NTA-AAm) possibly combined with heterogenous distribution of coumermycin (local coumermycin : GyrB ratios different from 1 : 2 (mol/mol) prevent efficient GyrB dimerization, Supplementary Fig. 3b). Heterogenous coumermycin distribution might be favored by precipitating antibiotic when added at the required high concentrations to the GyrB-poly(AAm-co-Ni^{2+}-NTA-AAm) mix as a 50 mg/ml stock solution in DMSO. Frequency sweep rheology experiments between 0.1-10 Hz revealed a marked frequency-dependence of the viscoelastic gel properties, in contrast to polymer networks crosslinked via covalent bonds that are nearly frequency-independent[20]. Notably, at higher frequencies (>7-8 Hz) a crossing over of G' and G'' was observed, indicating a reversion from a solid gel into a liquid state (Supplementary Figs. 5, 6, 7). The increase of the moduli at

higher frequencies is an indication of non-covalent "physical" crosslinks relaxing at higher frequencies.

Pharmacologically-triggered hydrogel formation and dissolution opens new perspectives for optimal delivery of protein-based pharmaceuticals within the body, provided that the dissolution kinetics of the hydrogel and the release properties of the biopharmaceutical can optimally be adjusted into the therapeutic window. In order to investigate adjustable hydrogel characteristics, we incubated coumermycin-crosslinked hydrogels in the presence of increasing novobiocin concentrations and followed gel dissolution by quantification of released GyrB-polymer complexes (Fig. 3a). In the presence of 1 mM novobiocin, the hydrogel dissolved rapidly whereas lower novobiocin concentrations correlated with slower hydrogel dissolution and slower GyrB release demonstrating adjustable dissolution and release kinetics (Fig. 3a). Apart from an initial protein release within the first few hours (Fig. 3a, probably due to non-efficiently incorporated GyrB), the hydrogel was stable for 24 days in the absence of novobiocin. Addition of 1 mM novobiocin at day 24 (+ Novo) resulted in dissolution of the hydrogel until day 26 demonstrating the long-term functionality of the hydrogel (Fig. 3b). Specificity to novobiocin was demonstrated by incubating the hydrogel in the presence of antibiotics of diverse classes (e.g. β-lactams (ampicillin), macrolides (erythromycin), aminoglycosides (gentamycin)), which did not impact on gel structure (data not shown).

In order to demonstrate pharmacologically-triggered release of a therapeutic protein from the stimuli-sensing hydrogel, we produced the human vascular endothelial growth factors 121 ($VEGF_{121}$[3]) incorporating a hexahistidine motiv at the N-terminus (sterical entrapment of proteins was not effective, Supplementary Fig. 8). $VEGF_{121}$ was incorporated into the hydrogel (GyrB : $VEGF_{121}$ = 1000:1, mol/mol of the active

$VEGF_{121}$ dimer) and incubated in the presence of increasing novobiocin concentrations (Fig. 4). In the presence of 1 mM novobiocin, $VEGF_{121}$ release reached a plateau within 10 h, while background $VEGF_{121}$ levels were observed in the absence of the stimulus after an initial short release of growth factor that was likely not well immobilized during the gelation process. At intermediate novobiocin concentrations (0.25 mM) $VEGF_{121}$ release kinetics were slower thereby demonstrating the trigger-adjustable growth factor release characteristics (Fig. 4). Biocompatibility of the material was validated by incubating different amounts of the $VEGF_{121}$-loaded and DMS-stabilized hydrogel (crosslinking ratio: 33±4 %) in the presence of the human model cell line, human embryonic kidney cells, for 48 h (hydrogels without additional DMS crosslinks were strongly swelling in DMEM medium so that they could hardly be handled any more). Although the gels contained sufficient $VEGF_{121}$ cargo to reach a final concentration of > 500 ng/ml (more than five to ten-fold excess to biologically-relevant saturating concentrations[21]), no cytotoxic effects could be observed as monitored by a proliferation-based cytotoxicity assay (Fig. 5a). Bioactivity and bioavailability of novobiocin-released $VEGF_{121}$ was monitored by incubating human umbilical vein endothelial cells (HUVEC[21]) for 96 h in the presence of cell culture medium containing $VEGF_{121}$-loaded hydrogel further supplemented with 0 or 200 μM novobiocin. In the presence of novobiocin, $VEGF_{121}$ was released resulting in significantly increased proliferation of HUVEC cells while in the absence of the release-inducing antibiotic no difference in proliferation could be observed as compared to the negative control without hydrogel, indicating that the non-specific leakage of non- or only weakly-bound $VEGF_{121}$ was not sufficient to produce a biologic effect. These novobiocin-triggered effects on $VEGF_{121}$ release in a cell culture environment and subsequent activation of proliferation of human primary

endothelial cells demonstrate the bioactivity and bioavailability of the released growth factor and underline the absence of cytotoxic side effects of released gel components.

In this study we have used for the first time pharmacologically controlled interactions between two proteins to design stimuli-responsive hydrogels for the release of a human growth factor in response to a clinically licensed stimulus. Novobiocin concentrations required for the release of a therapeutic protein out of the hydrogel can be maintained in the plasma over prolonged times ($t_{½}$ = 6h[22]), a clinical phase I study demonstrated that novobiocin concentrations above 0.15 mM were obtained for 24-72 h after a single oral dose[23]. Since novobiocin is mainly localized in the plasma, tissues well supplied with blood (e.g. muscle) would be the ideal localization of the hydrogel for trigger-inducible releasing its therapeutic cargo. Such trigger-adjustable release devices hold high potential in biomedical applications, since they could serve as economic and patient-compliant formulations for optimal administration of the rapidly growing number[24] of protein-based biopharmaceuticals.

Methods

Production of proteins, mammalian cell culture and analytics. Cloning of expression vectors for GyrB and $VEGF_{121}$ as well as the production, purification and characterization of the proteins is described in the Supplementary Information together with detailed information on mammalian cell culture techniques and analytical procedures.

Synthesis of 2,2'-(5-acrylamido-1-carboxypentylazanediyl)diacetic acid (NTA-AAm). 3.3 mmol acryloylchloride (ABCR, Karlsruhe, Germany, cat. no. AB172729)

dissolved in 15 ml toluene were drop wise added during 4 h to an ice-cooled solution of 3 mmol N,N-bis(carboxymethyl)-L-lysine (Fluka, Buchs, Switzerland, cat. no. 14580) dissolved in 27 ml 0.44 M NaOH. The toluene was evaporated *in vacuo* and sodium ions were removed with Dowex® 50WX8 (Acros, Geel, Belgium, cat. no. 335351000) prior to lyophilization resulting in a viscous oil (yield: 50 %) with a purity of 95 % as judged from ^{1}H NMR (Supplementary Fig. 1a).

^{1}H-NMR (Avance 500 Bruker BioSpin AG, Fällanden, Switzerland) (D_2O) δ, 1.43 (m, 2H, $CHCH_2C\underline{H}_2CH_2CH_2N$), 1.47 (m, 2H, $CHC\underline{H}_2CH_2CH_2CH_2N$), 1.89 (m, 2H, $CHCH_2CH_2C\underline{H}_2CH_2N$), 3.14 (t, 2H, $CHCH_2CH_2CH_2C\underline{H}_2N$), 4.11 (m, 1H, $C\underline{H}CH_2CH_2CH_2CH_2N$), 4.11 (s, 4H $NC\underline{H}_2COOH$), 5.61 (d, 1H, $CHC\underline{H}_2$), 6.03 (d, 1H, $C\underline{H}CH_2$), 6.11 (dd, 1H, $CHC\underline{H}_2$).

^{13}C-NMR (Avance 500 Bruker BioSpin AG, Fällanden, Switzerland) (D_2O) δ, 23.30 ($CHCH_2\underline{C}H_2CH_2CH_2N$), 27.02 ($CH\underline{C}H_2CH_2CH_2CH_2N$), 28.21 ($CHCH_2CH_2\underline{C}H_2CH_2N$), 39.12 ($CHCH_2CH_2CH_2\underline{C}H_2N$), 54.68 ($N\underline{C}H_2COOH$), 67.44 ($\underline{C}HCH_2CH_2CH_2CH_2N$), 127.45 ($CH\underline{C}H_2$), 130.43 ($\underline{C}HCH_2$), 168.91 ($NH\underline{C}O$), 169.95 ($CH_2\underline{C}OOH$), 171.43 ($CH\underline{C}OOH$).

ATR-IR (Bruker Optics IFS-66/S equipped with a liquid nitrogen-cooled MCT detector): 3261.1, 2941.0, 2869.6, 2522.5, 1729.9, 1650.8, 1562.1, 1417.5, 1355.7, 1201.5, 1066.5, 975.8, 891.0, 804.2.

MS (ES^+) (LCT, Waters AG, Baden-Dättwil, Switzerland) *m/z*: 317.5 [$M+H^+$].

Synthesis of poly(AAm-co-NTA-AAm). 1.5 mmol NTA-AAm and 6.4 mmol acrylamide (AAm, Pharmacia Biotech, Uppsala, Sweden, cat. no. 17-1300-01) were dissolved in 48 ml 50 mM Tris/HCl, pH 8.5 under nitrogen and polymerization was initiated by the addition of 150 µl ammonium peroxodisulphate (APS, 10%, w/v) and

24 µl N,N,N',N'-tetramethylethylenediamine (TEMED) for 20 h at room temperature. The polymer was concentrated to 20 ml *in vacuo* and subsequently dialyzed twice (3.5 kDa MWCO, Pierce, Rockford, IL, cat. no. 68035) against 2 l H_2O for 12 h to eliminate salts and low molecular weight compounds like residual acrylamide. The obtained molar ratio of AAm to NTA-AAm was 4 to 1 as determined by ^1H NMR (Avance 500 Bruker BioSpin AG Fällanden, Switzerland) (Supplementary Fig. 2b). The dialysate was supplemented with 3.5 mmol $NiSO_4$ and dialyzed twice against 0.5x PBS for 12 h and twice against 0.1x PBS for 12 h. The Ni^{2+}-charged polymer was concentrated 10-fold *in vacuo* resulting in a 6 % (w/v) solution. The size of Ni^{2+}-charged poly(AAm-co-NTA-AAm) was analyzed by gel permeation chromatography on Shodex OHpak SB-806 HQ and SB-804 HQ columns (both 8.0 mm x 300 mm) (Showa Denko, Kawasaki, Japan) in series, using 0.1 M $NaNO_3$ with 10% acetonitrile as mobile phase at a flow rate of 0.3 ml/min (Waters 2796 Alliance Bio). Detection was performed at 380 nm (Waters 996 PDA detector). As size standards, poly(styrenesulfonic acid sodium salt) (Fluka, Buchs, Switzerland) was used (Mp = 150 kDa (cat. no. 81614), 77 kDa (81612), 32 kDa (81610), 17 kDa (81609) and 6.8 kDa (81607)) which was detected at 260 nm.

Hydrogel formation. Purified GyrB (80 mg/ml) in PBS was mixed with coumermycin (50 mg/ml in DMSO) at a molar ratio of GyrB : coumermycin = 2:1 and incubated for 30 min at room temperature. Dimerized GyrB was subsequently added to 4.5 µl poly(AAm-co-Ni^{2+}-NTA-AAM) (as 6 % w/v solution in PBS) per mg GyrB and mixed by gently stirring. The hydrogel formed immediately and was incubated at 4 °C in a humidified atmosphere for 20 h prior to incubating the hydrogel for 12 h in PBS.

Hydrogel characterization. For investigation of trigger-inducible hydrogel dissolution, the gel was incubated in PBS in the presence of different novobiocin (Fluka, cat. no. 74675) concentrations and the dissolution was monitored optically (GelJet Imager 2004, Intas, Göttingen, Germany) and by quantification of GyrB release into the buffer using the Bradford method. Error bars represent the standard deviation from three experiments. Swelling of hydrogels was quantified by synthesizing micro dome-shaped gels (14 µl/gel) on siliconized (Sigmacote, Sigma, St. Louis, MO, cat. no. SL-2) glass slides and optical analysis of the gel size using a Leica DM-RB microscope (Leica, Wetzlar, Germany) with built-in scale bar (assuming isotropic swelling). Details for the rheology measurements are shown in the Supplementary Information.

References

1. Farrar, M. A., Alberol, I. & Perlmutter, R. M. Activation of the Raf-1 kinase cascade by coumermycin-induced dimerization. *Nature* **383**, 178-81 (1996).
2. Hacker, H. *et al*. Specificity in Toll-like receptor signalling through distinct effector functions of TRAF3 and TRAF6. *Nature* **439**, 204-7 (2006).
3. Ehrbar, M. *et al*. Cell-demanded liberation of VEGF121 from fibrin implants induces local and controlled blood vessel growth. *Circ Res* **94**, 1124-32 (2004).
4. Denhardt, D. T. DNA gyrase and DNA unwinding. *Nature* **280**, 196-8 (1979).
5. Ehrick, J. D. *et al*. Genetically engineered protein in hydrogels tailors stimuli-responsive characteristics. *Nat Mater* **4**, 298-302 (2005).
6. Lendlein, A., Jiang, H., Junger, O. & Langer, R. Light-induced shape-memory polymers. *Nature* **434**, 879-82 (2005).
7. Miyata, T., Asami, N. & Uragami, T. A reversibly antigen-responsive hydrogel. *Nature* **399**, 766-9 (1999).
8. Wang, C., Stewart, R. J. & Kopecek, J. Hybrid hydrogels assembled from synthetic polymers and coiled-coil protein domains. *Nature* **397**, 417-20 (1999).

9. Thornton, P. D., McConnell, G. & Ulijn, R. V. Enzyme responsive polymer hydrogel beads. *Chem Commun (Camb)* **47**, 5913-5 (2005).

10. Lutolf, M. P. *et al.* Repair of bone defects using synthetic mimetics of collagenous extracellular matrices. *Nat Biotechnol* **21**, 513-8 (2003).

11. Um, S. H. *et al.* Enzyme-catalysed assembly of DNA hydrogel. *Nat Mater* **5**, 797-801 (2006).

12. Toledano, S., Williams, R. J., Jayawarna, V. & Ulijn, R. V. Enzyme-triggered self-assembly of peptide hydrogels via reversed hydrolysis. *J Am Chem Soc* **128**, 1070-1 (2006).

13. Murakami, Y. & Maeda, M. DNA-responsive hydrogels that can shrink or swell. *Biomacromolecules* **6**, 2927-9 (2005).

14. Kopecek, J. Smart and genetically engineered biomaterials and drug delivery systems. *Eur J Pharm Sci* **20**, 1-16 (2003).

15. Lutolf, M. P. & Hubbell, J. A. Synthetic biomaterials as instructive extracellular microenvironments for morphogenesis in tissue engineering. *Nat Biotechnol* **23**, 47-55 (2005).

16. Beebe, D. J. *et al*. Functional hydrogel structures for autonomous flow control inside microfluidic channels. *Nature* **404**, 588-90 (2000).

17. Clardy, J., Fischbach, M. A. & Walsh, C. T. New antibiotics from bacterial natural products. *Nat Biotechnol* **24**, 1541-50 (2006).

18. Gormley, N. A., Orphanides, G., Meyer, A., Cullis, P. M. & Maxwell, A. The interaction of coumarin antibiotics with fragments of DNA gyrase B protein. *Biochemistry* **35**, 5083-92 (1996).

19. Winter, H. H. & Chambon, F. Analysis of Linear Viscoelasticity of a Crosslinking Polymer at the Gel Point. *J. Rheol*. **30**, 367-382 (1986).

20. Lutolf, M. P. & Hubbell, J. A. Synthesis and physicochemical characterization of end-linked poly(ethylene glycol)-co-peptide hydrogels formed by Michael-type addition. *Biomacromolecules* **4**, 713-22 (2003).

21. Ehrbar, M., Metters, A., Zammaretti, P., Hubbell, J. A. & Zisch, A. H. Endothelial cell proliferation and progenitor maturation by fibrin-bound VEGF variants with differential susceptibilities to local cellular activity. *J Control Release* **101**, 93-109 (2005).

22. Eder, J. P., Wheeler, C. A., Teicher, B. A. & Schnipper, L. E. A phase I clinical trial of novobiocin, a modulator of alkylating agent cytotoxicity. *Cancer Res* **51**, 510-3 (1991).

23. Murren, J. R. *et al.* Phase I and pharmacokinetic study of novobiocin in combination with VP-16 in patients with refractory malignancies. *Cancer J* **6**, 256-65 (2000).

24. Aggarwal, S. What's fueling the biotech engine? *Nat Biotechnol* **25**, 1097-104 (2007).

Acknowledgements

We are grateful to Matthias Lütolf for his critical comments on the manuscript as well as his advice on the rheology measurements. We thank Bettina Keller for cloning plasmid pWW873, Ronny Wirz for IR spectra analysis, Samy Gobaa for expertise in rheology measurements, Markus Rimann for providing HUVEC cells and Jens Loebus for technical assistance. The project has been made possible thanks to start-up financing by the GEBERT RÜF STIFTUNG (Grant No. GRS-042/07) to Wilfried Weber.

Competing interests statement

ETH Zurich has filed an application for a patent on the technology described in this manuscript, of which M.F. and W.W. are inventors.

Figure legends

Figure 1: Design of pharmacologically-controlled hydrogels **(a)** Bacterial gyrase subunit B (GyrB) coupled to an acrylamide polymer is dimerized by coumermycin (+ Coumermycin) resulting in gelation of the hydrogel. In the presence of novobiocin (+ Novobiocin) GyrB is dissociated resulting in dissolution of the hydrogel. **(b)** Coupling of proteins to the acrylamide polymer. Polyacrylamide is functionalized with nitrilotriacetic acid chelating a Ni^{2+} ion to which GyrB can bind via a hexahistidine sequence.

Figure 2: Synthesis and characterization of pharmacologically-controlled hydrogels. **(a)** Antibiotic-dependent hydrogel formation. His-tagged GyrB was incubated with coumermycin (GyrB:coumermycin = 2:1, mol/mol), novobiocin (GyrB:novobiocin = 1:10, mol/mol) or without any antibiotic (w/o) prior to the addition of poly(AAM-co-Ni^{2+}-NTA-AAM). Following 12 h incubation, PBS was added and released GyrB was quantified after another 12 h. **(b)** Hydrogels were formed as described in Fig. 2a with coumermycin-dimerized GyrB, which was further covalently crosslinked with equimolar amounts of dimethylsuberimidate (+ DMS, crosslinking ratio: 33±4 %). Following swelling over night in PBS, the hydrogels were placed in PBS containing 1 mM novobiocin and released GyrB was quantified. **(c)** Antibiotic-dependent swelling of DMS-stabilized hydrogels. DMS-stabilized hydrogels were prepared as described above (Fig. 2b) and incubated in the presence or absence of novobiocin (1 mM). Changes in size were monitored microscopically. **(d)** Viscoelastic properties of hydrogels. Hydrogels were prepared by first dimerizing GyrB with coumermycin and subsequent mixing with poly(AAm-co-Ni^{2+}-NTA-AAm) (G-C-G + poly) or GyrB was first mixed with poly(AAm-co-Ni^{2+}-NTA-AAm) prior to the addition of coumermycin (G-poly + C). Alternatively, DMS-crosslinked gels (G-C-GxDMS + poly) were used as described in Fig. 2b. The gels were swollen in PBS over night and the storage and the loss moduli G' and G'' were determined at 1.1 Hz.

Figure 3: Adjustable pharmacologically triggered disintegration of the hydrogel. **(a)** Hydrogels were synthesized from (per ml hydrogel) 57.4 mg GyrB (2.1 µmol, used at 80 mg/ml in PBS), 1.17 mg coumermycin (1.05 µmol, used at 50 mg/ml in DMSO) and 15.5 mg poly(AAm-co-Ni^{2+}-NTA-AAM) (used at 6 % (w/v) in PBS). For synthesis, GyrB was dimerized with coumermycin for 30 min prior to mixing with

poly(AAm-co-Ni^{2+}-NTA-AAM) and subsequent incubation for 20 h and a 12 h swelling period in PBS. Hydrogels were then incubated in new PBS in the presence of different novobiocin concentrations (0 - 1 mM) and hydrogel disintegration was measured by quantification of GyrB released into the buffer. **(b)** Long-term stability of the hydrogel. The hydrogel was incubated in PBS for 24 days prior to the addition of 1 mM novobiocin.

Figure 4: Antibiotic-inducible release of $VEGF_{121}$. Hydrogels were synthesized as described in Fig. 3 except that hexahistidine-tagged $VEGF_{121}$ (1 mmol/mol GyrB, as 20 µg/µl stock solution) was added to the dimerized protein prior to mixing with poly(AAm-co-Ni^{2+}-NTA-AAM). The hydrogels were incubated for 24 h and subsequently swollen in PBS for another 48 h. The hydrogels were then incubated in the presence of increasing novobiocin concentrations and $VEGF_{121}$ release into the buffer was followed over time.

Figure 5: Biocompatibility of pharmacologically-triggered hydrogels and bioavailability of the cargo growth factor. **(a)** Biocompatibility of the hydrogels. Hydrogels with incorporated $VEGF_{121}$ were prepared as described in Fig. 4 except that GyrB was further chemically crosslinked with equimolar amounts of dimethylsuberimidate for 1 h. Gels of different size were incubated for 20 h, swollen for another 24 h in DMEM medium containing 10 % FCS and subsequently incubated in the presence of human embryonic kidney cells (120'000 cells/ml) for another 48 h prior to quantification of cell proliferation. The grey range indicates the proliferation in the absence of any gel +/- 1 standard deviation (derived from 9 replicates). **(b)** Bioavailability and bioactivity of released $VEGF_{121}$. Hydrogels as prepared in Fig. 5a

were incubated in DMEM medium containing 10 % FCS in the presence or absence of 200 μM novobiocin for 24 h. The supernatant containing the released $VEGF_{121}$ (and dissolved gel components) was subsequently added to HUVEC cells and incubated for 96 h prior to quantification of cell proliferation. As control, HUVEC cells were incubated in the absence of any hydrogel (w/o).

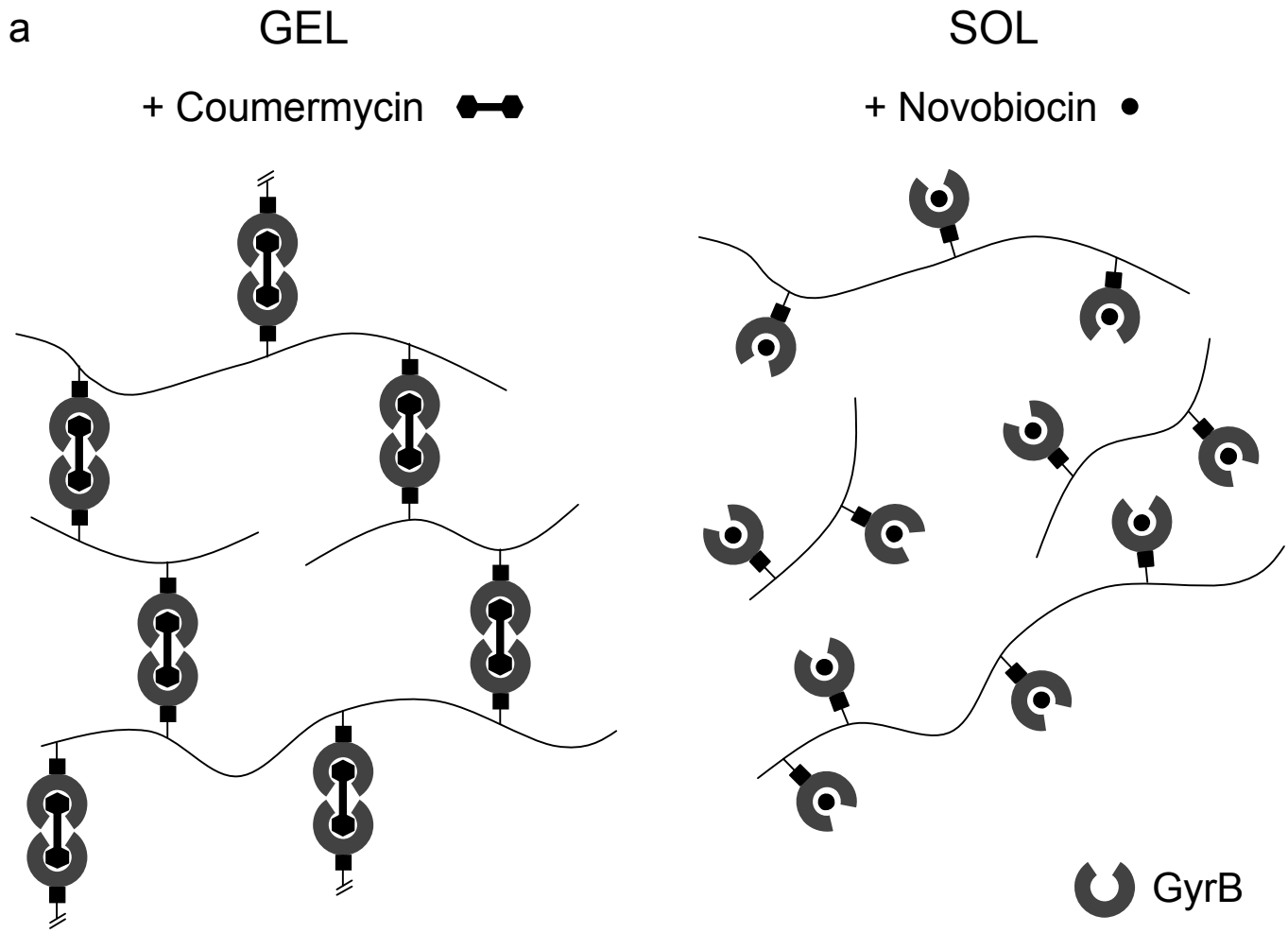

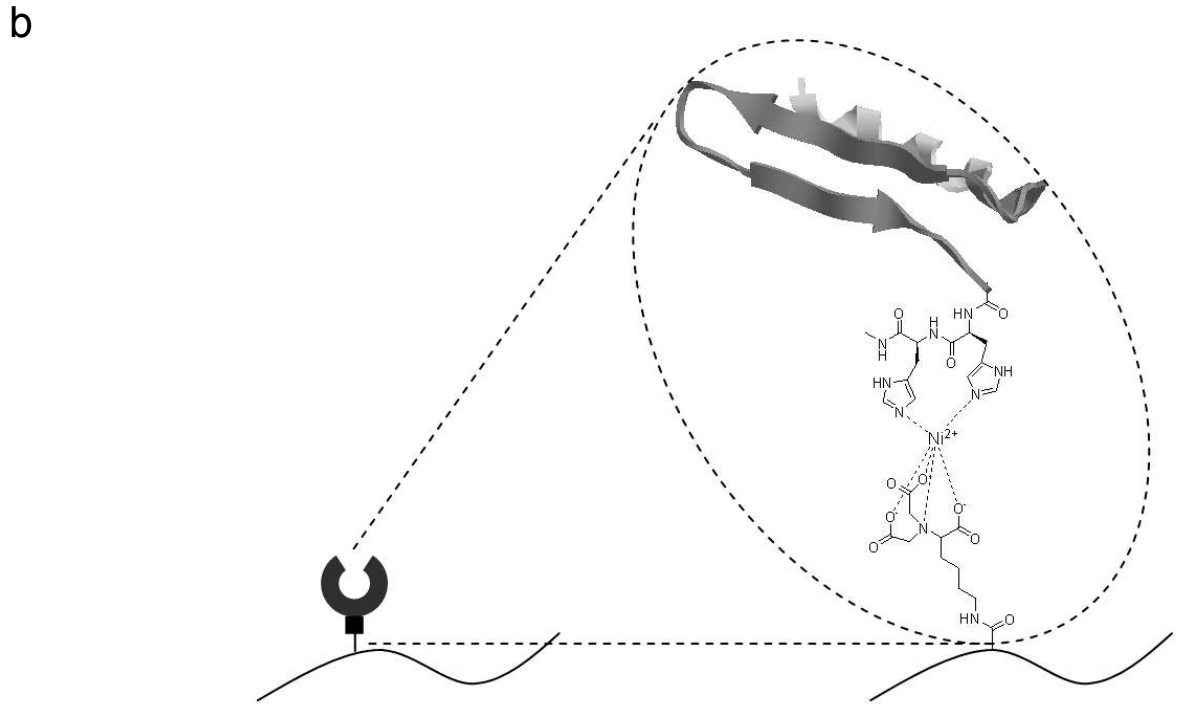

Figure 1

a

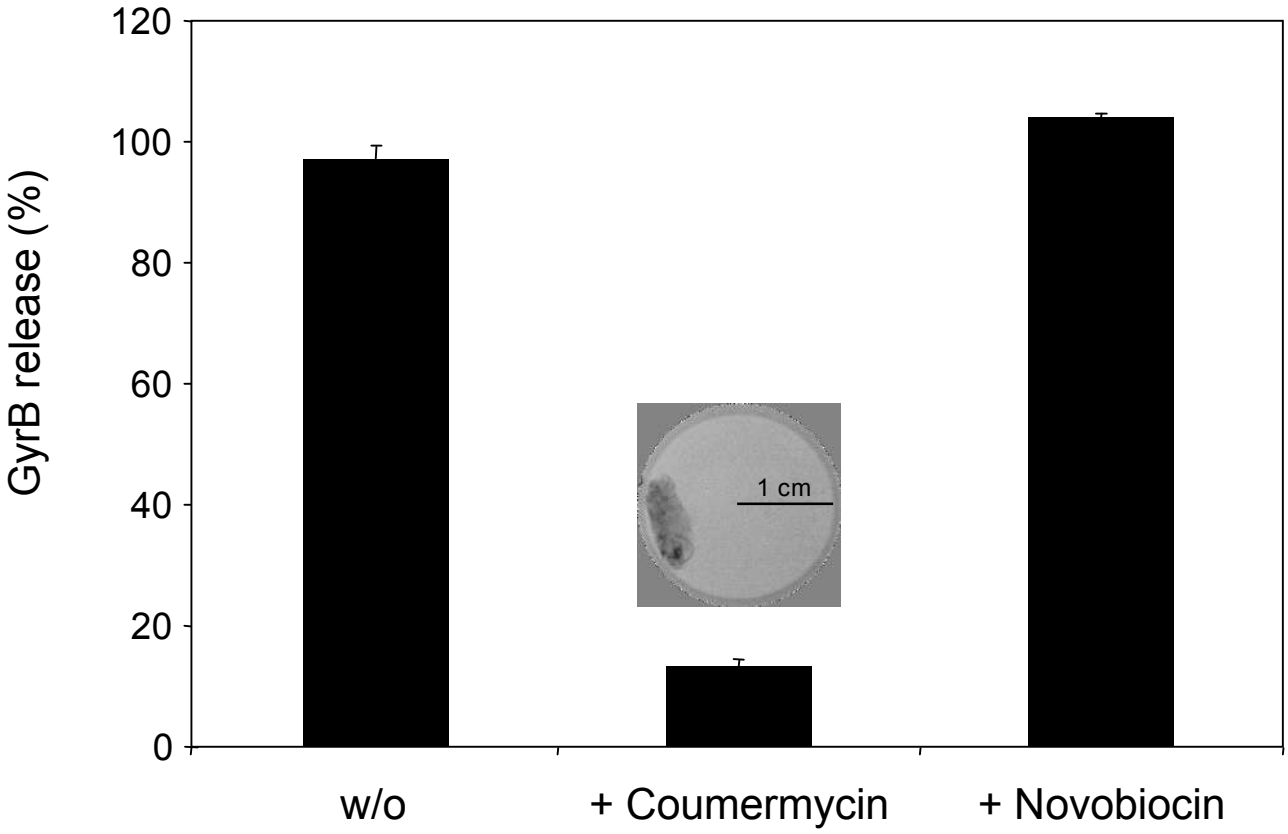
GyrB release (%)
120
100
80
60
40
20
0
1 cm
w/o
+ Coumermycin
+ Novobiocin

b

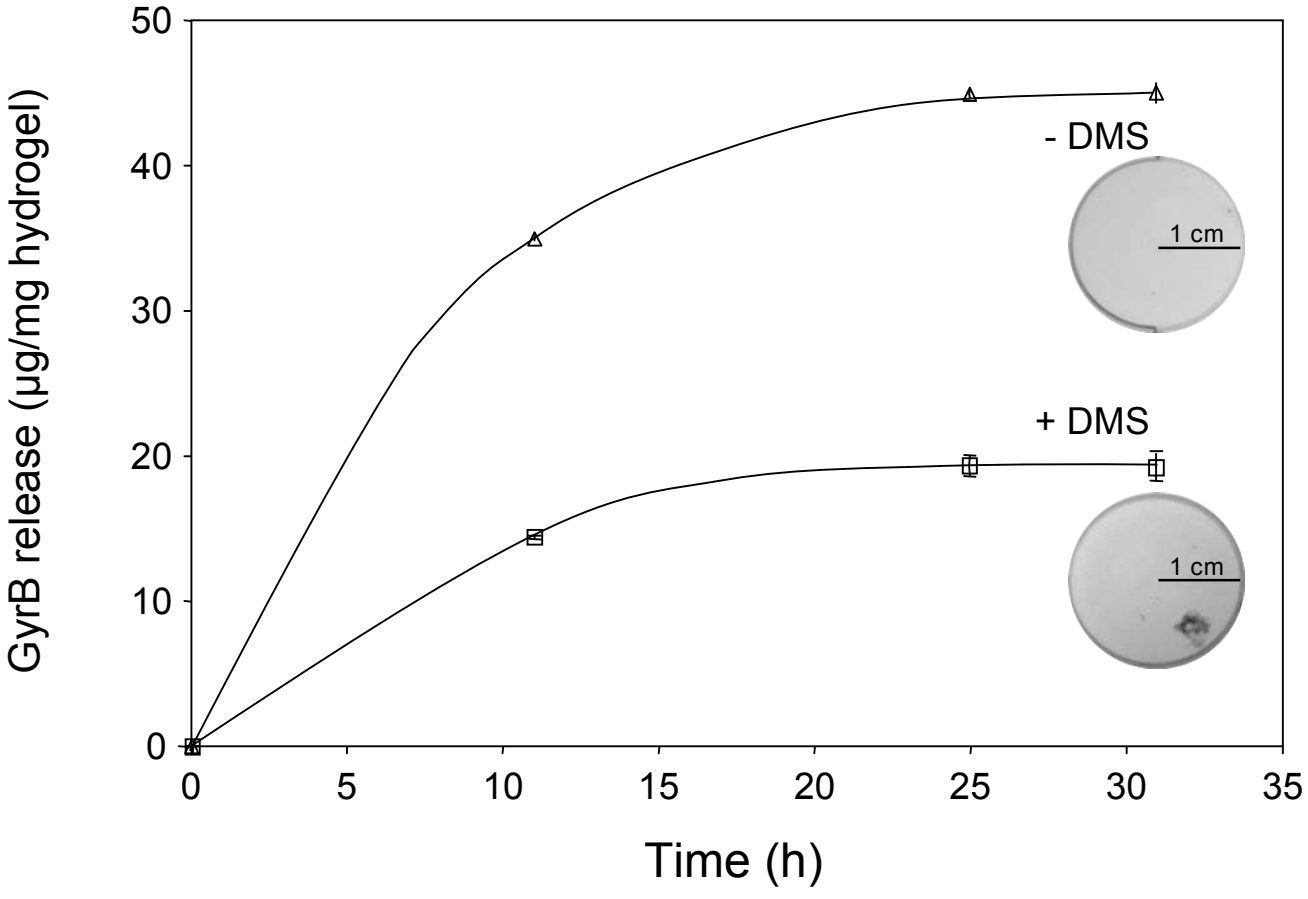
GyrB release (µg/mg hydrogel)
50
40
30
20
10
0
- DMS
1 cm
+ DMS
1 cm
0
5
10
15
20
25
30
35
Time (h)

Figure 2

a

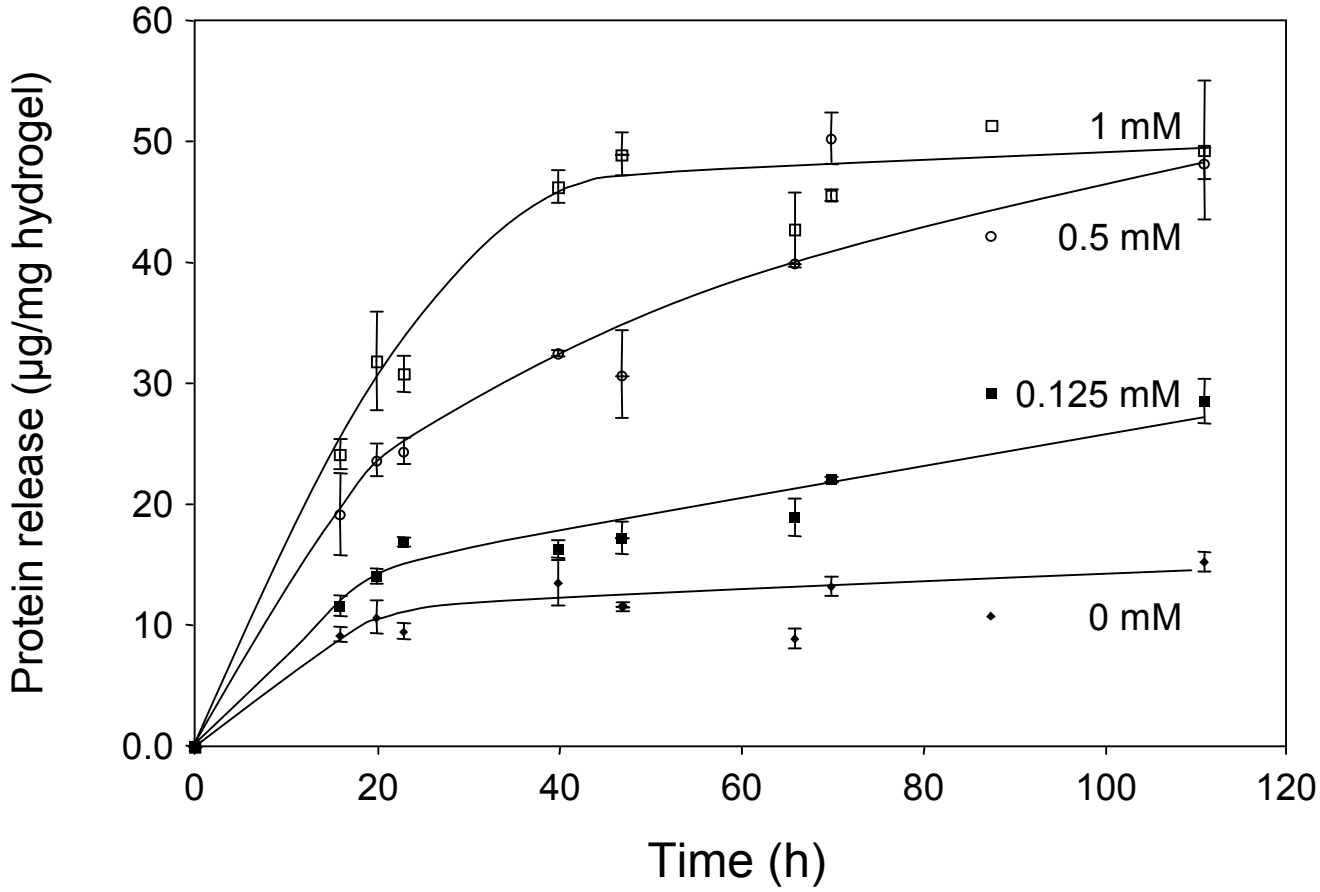
Protein release (µg/mg hydrogel)
Time (h)
1 mM
0.5 mM
0.125 mM
0 mM
0.0
10
20
30
40
50
60
0
20
40
60
80
100
120

b

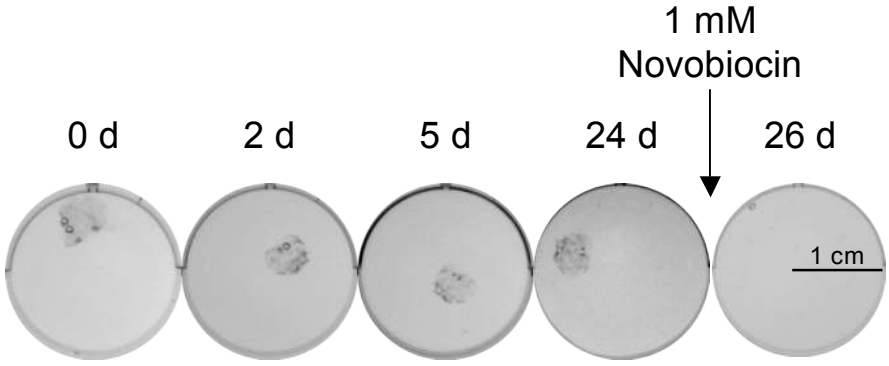
1 mM
Novobiocin
0 d
2 d
5 d
24 d
26 d
1 cm

Figure 3

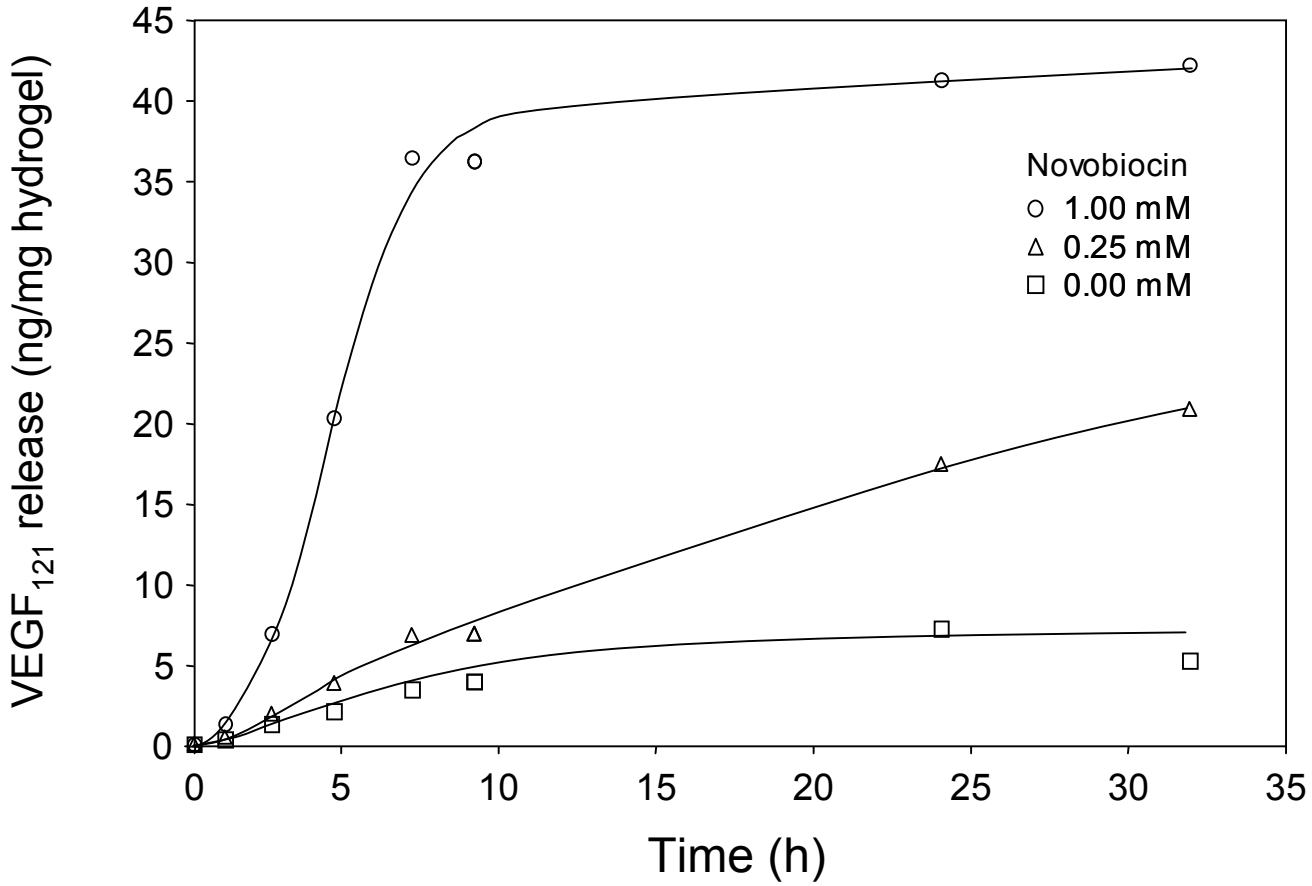
VEGF121 release (ng/mg hydrogel)
Time (h)
Novobiocin
1.00 mM
0.25 mM
0.00 mM
0
5
10
15
20
25
30
35
40
45

Figure 4